IOP Publishing

Exocytosis: From Molecules to Cells

Arun Anantharam and Jefferson Knight

Chapter 5

Fusion pore stability and dynamics

Meyer B Jackson

During exocytosis, secretion is initiated by the formation of a fusion pore that serves as a fluid conduit between the vesicle lumen and extracellular space. Fusion pore properties can be measured in real time by a variety of sensitive biophysical techniques. These measurements reveal the evolution of a fusion pore as it expands, contracts, and closes. These dynamic processes have important functional implications for control of the speed, extent, and composition of secretion. This chapter focuses on the diversity of fusion pore states and the dynamics of their interconversion. The investigations into these processes have illuminated the molecular drives and controls of exocytosis, and revealed the mechanisms by which fusion pores adapt to meet diverse biological challenges.

The fusion pore serves as an essential exit pathway for secretion. Its critical function makes the fusion pore a natural focus of research in exocytosis. The fusion pore has provided a window into the mechanisms by which proteins drive membrane fusion, and has provided a framework for defining intermediate states with distinct functions. Secretion begins with the opening of a fusion pore, but because the initial pore is very narrow, only small molecules can escape at a very slow rate. The nascent fusion pore can undergo dynamic transitions, which are essential for most of the biological functions of exocytosis. Fusion pores can expand, constrict, and close to shape a chemical signal and determine the biological outcome. Exocytosis can reach an endpoint of full fusion, in which a fusion pore expands to expel a vesicle's entire content, perhaps accompanied by collapse of the vesicle membrane into the plasma membrane. Alternatively, exocytosis can terminate in kiss-and-run, in which a vesicle maintains its integrity and releases a fraction of its content before the fusion pore closes.

Fusion pore researchers initially looked for general features and focused on common properties. However, it quickly became clear that fusion pores are very diverse. Not only do estimates of size vary widely, but the size can fluctuate. Fusion pores interconvert between states with different properties that enable different

doi:10.1088/978-0-7503-3771-7ch5

forms of secretion. Fusion pore dynamics defines a spectrum of potential outcomes. Exocytosis is tuned and regulated by controlling which fusion pore structures form and how they interconvert. The fusion pore should be viewed as a dynamic entity moving along a kinetic reaction pathway. Studying the trajectory of a fusion pore along this pathway illuminates many of the biological controls of secretion. This chapter considers the diversity of fusion pore states, the kinetics of interconversions, and the functional consequences.

5.1 Techniques for studying fusion pores

Different experimental techniques have provided pictures of fusion pores in living cells. A number of these techniques can measure signals arising from single vesicles, so they can be viewed as probing fusion pores at the unitary, 'single-channel' level. Unitary measurements have the advantage of directly visualizing molecular heterogeneity, which is generally obscured in measurements of ensemble averages. Single fusion pore measurements have the additional advantage that they can be connected to a molecular dimension to estimate the pore size. Different measurements focus on characteristic timescales, capturing fusion pores at particular stages in their evolution. This makes it hard to compare the fusion pore dimensions inferred by different methods. The brief survey of techniques given here will emphasize the nature of the information they provide, and how they have revealed heterogeneity and dynamics. Discussions of function, energetics, and transitions will then synthesize the results obtained with different methods and consider the broader framework.

Electrical recording. Phase-locked impedance measurements revealed stepwise increases in capacitance as single vesicles fused. Some upward steps were immediately followed by downward steps, as though a pore was flickering open and closed [1, 2]. This was reminiscent of ion-channel gating transitions and anticipated the advent of fusion pores. The complex impedance of a membrane could be resolved into in-phase and out-of-phase components, and the fusion of giant vesicles in beige mouse mast cells changed both components. With the aid of an equivalent circuit, the fusion pore conductance was then calculated from these measurements [3]. At the instant when these large vesicles fused, they produced a distinct current transient as the vesicle membrane potential discharged, and analysis in terms of the equivalent circuit yielded a time course for fusion pore expansion [4].

Of all the fusion pore measurements, conductance comes the closest to measuring the physical size. However, these estimates generally depend on assuming the pore has a cylindrical geometry, with a length that spans two lipid bilayers. Applying the formula for a cylinder to ion channels with known structures gives reasonable values for pores with diameters >1 nm, but fails badly for smaller channels [5]. The cylindrical approximation also breaks down for very large pores when high fluxes create concentration gradients around the pore. In this case, the flux scales with the pore diameter rather than the area [5–7]. Proteinaceous pores are more likely to be cylindrical, but lipid bilayer elasticity opposes the formation of sharp corners. Lipidic pores are presumed to form a shape that minimizes the elastic bending

energy of a lipid bilayer [8]. Modeling of lipid bilayer elasticity indicates that lengthening a pore and reducing the meridian curvature lowers the membrane bending energy. These 'bowed' or 'teardrop' pores are approximately cylindrical [9, 10]. The cylindrical model may be a good approximation for the flux through this form of lipidic pore. It would be useful to know more about how physical forces shape the fusion pore, but experimental studies are not currently able to address this question.

The cylindrical model has probably been overused, but it is the best we have at this stage. These limitations should be borne in mind when considering pore dimensions estimated from conductance. Fusion pore conductances range from tens of picosiemens to a few nanosiemens [11], and the inferred diameters range from a few Angstroms to a few nanometers. Fusion pores associated with small synaptic-like vesicles have conductances about tenfold smaller than fusion pores associated with large endocrine vesicles [12]. The wide range of conductance values reported in the literature [11] speaks to the range of sizes fusion pores can assume. In summary, complex impedance measurements have provided insight into the dimensions of pores and revealed rich dynamic behavior. Impedance measurement is, however, not the fastest technique and cannot resolve rapid dynamic processes beyond the millisecond timescale.

Amperometry. Some secreted molecules, such as catecholamines and serotonin, oxidize upon contact with a carbon fiber electrode polarized to a degree greater the molecule's redox potential. This oxidization provides a signal for the electrochemical detection of these molecules. Carbon fiber electrodes with ~5 μm tips positioned at the surface of a cell detect catecholamine release as an amperometric current, and the fusion of a single vesicle produces a large, rapid, spike-like event [13]. Close inspection of single-vesicle spikes has revealed that they often begin with a small foot. This prespike foot represents the opening of a fusion pore, and ends with a spike as the fusion pore abruptly expands [14, 15]. The prespike foot is probably the earliest measurable signal of a fusion pore, and thus provides the clearest view of the nascent fusion pore. Mutations in a variety of proteins alter their permeability and stability [16]. Mutations in the soluble *N*-ethylmaleimide-sensitive factor attachment receptor (SNARE) protein transmembrane domains (TMDs) alter fusion pore flux in a manner suggesting that these domains line the nascent fusion pore [17–19] (see figure 5.3).

After the onset of a spike, the impact of a fusion pore becomes more difficult to discern. The time course of the spike cannot be accounted for by diffusion of the escaping catecholamine to the electrode surface [20]. Dissociation from the protein matrix within a dense-core vesicle has been considered to be a potential factor in slowing catecholamine loss [21, 22]. However, the various contributions of diffusion, dissociation, and fusion pore dynamics have been difficult to resolve. A method of analysis of amperometry spikes has been developed that offers a window into the dynamics of pore permeability [23]. One begins by integrating the amperometric current to obtain the amount of catecholamine lost before a given time. The number of molecules remaining in the vesicle is then calculated as the initial number minus the number lost. The concentration gradient through the pore can be taken to be the

intravesicular concentration, because the extracellular concentration is very small. Thus, the number of moles remaining in the vesicle divided by the vesicle volume represents the driving force for the flux. Dividing amperometric current by this driving force gives the fusion pore permeability over the vesicle volume. This permeability can be calculated over the course of a spike to reveal rapid fusion pore dynamics (permeability/volume = α/V in figure 5.1). α/V increases rapidly at the end of a prespike foot, reaches a peak, and declines, before settling into a plateau that lasts tens of milliseconds. In this way amperometry can be used to probe the dynamic behavior of a fusion pore over the course of the spike.

Fluorescence destaining. Fluorescent dye and fluorescent cargo can label vesicles, and when a vesicle fuses, the fluorescence from the label declines. In synaptic vesicles the destaining of the lipid probe FM1–43 can be resolved into quantal steps corresponding to the fusion of single vesicles [24]. In a study of goldfish retinal neurons using total internal reflection fluorescence (TIRF) microscopy, vesicles destained completely in a few milliseconds, suggesting that the fusion pore expanded so rapidly that dye could escape unimpeded [25]. However, in hippocampal nerve terminals, a significant fraction of events were subquantal, and dye loss was

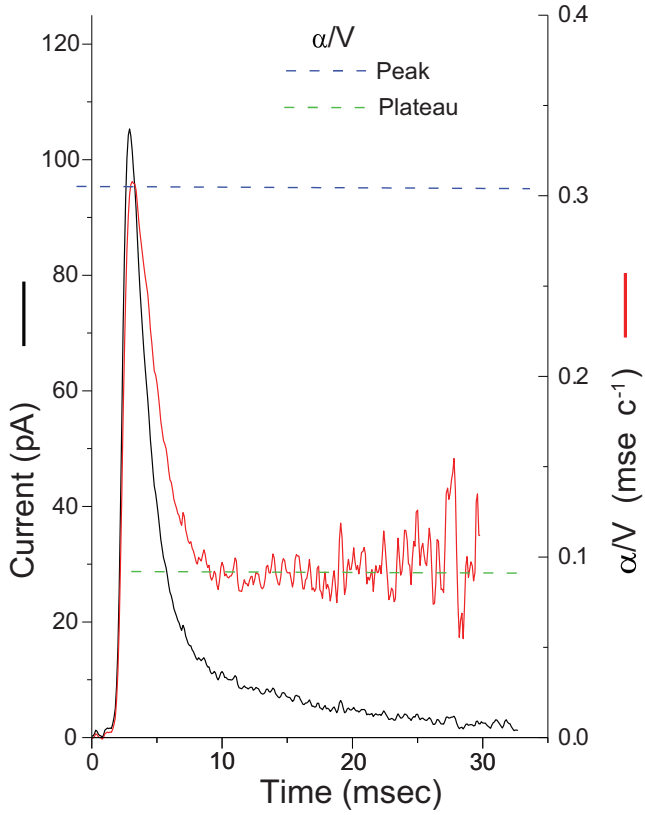

Figure 5.1. Amperometry current (black) and permeability (α/V, red). Permeability rises rapidly and then falls, settling to a stable plateau. Reproduced from [23]. Copyright 2000 Biophysical Society.

markedly slower [26, 27]. The slow events suggested dye loss by a process similar to that seen in liposomes containing ion channels. These events appeared to originate from exit through a stable fusion pore with a diameter of 1–2 nm [27]. Thus, single-vesicle fluorescence destaining measurements reveal two distinct modes of synaptic vesicle fusion, namely slow graded release through small fusion pores and rapid complete release through rapidly expanding fusion pores.

Dual fluorophore experiments permitted the simultaneous monitoring of cargo loss and membrane loss [28]. Vesicles lost the lipid label FM4–64 but retained the cargo enhanced green fluorescent protein (EGFP)-phogrin, indicating that the fusion pore closed after expanding to a lipidic state. Large hormones can remain within endocrine vesicles for seconds after the onset of fusion. This process, referred to as 'cavicapture,' indicates the presence of a narrow fusion pore that is stable for seconds [29].

Polarization TIRF. The perpendicular and in-plane components of polarization can be separated in TIRF, and the ratio of the two provides a signal closely related to the amount of lipid bilayer curvature at the site of fusion [30]. This technique revealed an increase in membrane curvature that occurred at the onset of loss of cerulean fluorescent protein-tagged neuropeptide Y (NPY). Increases prior to the onset of content loss report membrane deformations during, or in preparation of, nascent fusion pore opening [31]. Membranes became curved at the site of release within a few hundred milliseconds of the onset of cargo loss. Since high membrane curvature is a hallmark of a lipidic fusion pore, this technique links the lipidic pore to the efflux of peptide cargo.

Super-resolution microscopy. Stimulated emission depletion (STED) microscopy has been used to visualize the vesicle and plasma membrane in real time as fusion takes place [32, 33]. With a time resolution of ~30–100 ms and a spatial resolution of 65–150 nm, this technique follows the formation and expansion of omega-shaped figures and tracks the movement of plasma membrane label through the fusion pore and into the vesicle. STED microscopy reveals fusion pores at a very late stage after they have grown quite large (to a size of tens of nanometers). The technique lacks the temporal and spatial resolution to see the smaller, briefer pores observed with complex impedance and amperometry, which are estimated to have sizes of 1 nm or less. STED microscopy has revealed an especially rich dynamic repertoire of fusion pores with a wide range of trajectories. Pores expand and constrict; some vesicles preserve their integrity, while others collapse into the plasma membrane.

STED microscopy tracks aqueous and membrane labels and has the potential to test hypothetical mechanisms. During some fusion events, a label of the intracellular membrane face moved to vesicles before a label of the extracellular membrane face, and before a change in pH of the vesicle lumen [32]. The formation of a hemifusion diaphragm prior to fusion pore opening can account for this result. To label the inner surface of the plasma membrane, these results employed a green fluorescent protein (GFP)-tagged pleckstrin homology domain, which binds phosphatidylinositol 4,5-biphosphate (PIP_2). Abbineni *et al* [34] have pointed out that this reagent can inhibit exocytosis, further noting that Ca^{2+}-triggered PIP_2 synthesis on vesicles and the dynamics of this reagent's binding could lead to labeling of vesicles without diffusion through contiguous lipid monolayer.

Unitary synaptic release. The spontaneous fusion of a single synaptic vesicle elicits a miniature postsynaptic current (mPSC) that can be seen in whole-cell patch clamp recordings from a postsynaptic cell. In these single-vesicle fusion events, the postsynaptic receptor reports the time course of release, but because synaptic transmission is fast and dependent upon a sequence of rapid events, it is difficult to extract information about fusion pores from mPSCs. Molecular manipulations of the exocytotic apparatus of a nerve terminal alter the shape of an mPSC, suggesting that fusion pores control synaptic release [35–37]. Tryptophan substitutions in the TMD of synaptobrevin slow mPSCs in a manner consistent with a reduction in transmitter flux through the synaptic fusion pore (see figure 5.3) [38], and these effects are clearer in artificial synapses formed between neurons and human embryonic kidney (HEK) cells expressing appropriate postsynaptic proteins [39]. Modeling of synaptic release indicates that fusion pores must expand very rapidly to raise subsynaptic neurotransmitter concentrations to sufficient levels to activate ionotropic receptors [16, 40–43]. This aspect of fusion pore dynamics is functionally critical, but at present there are no direct observations of synaptic fusion pores. The mPSCs associated with kiss-and-run are clearly slower, indicating that when fusion pores fail to expand, the rate and extent of postsynaptic receptor activation are reduced [44, 45].

Nanodiscs. To study fusion pores *in vitro*, investigators have developed systems with proteins reconstituted into lipid bilayer membranes [46–48]. This enables the study of fusion in a system of defined composition using membranes containing recombinant proteins. Nanodiscs have emerged as an especially powerful reconstituted system for fusion pore studies. These small 6–50 nm lipid bilayer disks are surrounded by a membrane scaffold protein to protect the hydrophobic core at the edges from water [48, 49]. With nanodiscs one can control not only the protein composition but also the copy number. Nanodiscs containing SNARE proteins fuse with cells expressing reverse-oriented cognate SNAREs [50, 51], as well as with SNARE-containing black lipid bilayer membranes [37, 52]. In both cases, robust fusion pore signals were observed. The direct measurement of single-channel ionic current provides the highest resolution of fusion pore dynamics currently achievable, and reveals rapid opening and closing transitions reminiscent of ion-channel gating. However, the finite size of a nanodisc limits fusion pore expansion and leaves late-stage fusion pores out of reach.

5.2 Functional considerations

As fusion pores grow, constrict, and close, the speed and composition of secretion change. The distinct properties of fusion pore states have many important functional consequences.

Flux. Fusion pores control the speed with which molecules escape from a vesicle. Size has an obvious impact: larger pores support higher fluxes. The cylindrical pore discussed above in the context of conductance measurements is expected to produce a flux that is proportional to the area and inversely proportional to the length. A high flux produces a steep gradient outside the fusion pore, which creates high local

concentrations at the pore mouth. If a secreting cell has receptors for the molecules it is releasing, then rapid flux can raise concentrations locally to activate these autoreceptors. Receptors activated cooperatively by multiple ligands are especially sensitive to a high local concentration created by high pore flux. If the cell surface has processing enzymes, high fluxes may saturate local catalytic sites and allow more substrate molecules to escape unchanged.

If surrounding extracellular structures impede escape, as in a synaptic cleft, then this transient confinement amplifies the impact of high flux. Local concentrations can then rise to a level sufficient to activate postsynaptic receptors. Rapid fusion pore flux is essential for the activation of ionotropic synaptic receptors, which generally require the binding of two or more ligands. This cooperative activation often depends on neurotransmitter concentrations reaching 10–100 μM. Modeling studies suggest that to achieve such concentrations, synaptic fusion pores must expand to diameters of several nanometers within ~50 μs of opening [16, 41]. If expansion is too slow then neurotransmitter diffuses away without reaching a high subsynaptic concentration, essentially losing the opportunity to activate postsynaptic receptors. At synapses, flux has a major impact on function, setting a requirement for fusion pore size, and for rapid expansion to reach that size.

Molecular size and filtering. Vesicles contain molecules varying in size from ~100 D for small neurotransmitters to ~100,000 D for large peptide hormones. Their molecular dimensions thus vary from a few Angstroms to nearly 10 nm. Molecules that are larger than a fusion pore cannot escape and are not secreted. Thus, fusion pores filter vesicle contents. This can serve as a very important form of biological control by determining the composition of a secretion. With vesicles containing mixed cargo, a stimulus can trigger the release of different molecules in different proportions by effecting the formation of small or large fusion pores [53, 54].

Charge selectivity. Molecular interactions between the secreted molecules and the surrounding pore could impact fusion pore flux, as is well documented for ion permeation through ion channels. Small fusion pores have been reported to show selectivity for cations over anions [55]. The selectivity is modest compared to that of ion channels, but nevertheless favors flux of cations such as catecholamines and acetylcholine over anions such as glutamate. As pores dilate they lose this selectivity.

Closure and kiss-and-run. Fusion pores can close to terminate an exocytotic event, in a process generally referred to as kiss-and-run. This results in subquantal release. If a fusion pore closes without reaching a size large enough for the passage of high-molecular-weight peptides, then only small molecules can escape. Fusion pores can close after reaching quite large sizes [56], in which case large cargoes can also escape. Kiss-and-run represents a distinct and well-defined mode of release, which at synapses produces synaptic potentials that are smaller and slower [44, 45].

Chemistry. The smallest nascent fusion pore can still allow virtually instantaneous equilibration of protons between the vesicle lumen and extracellular fluid. Thus, fusion pore opening produces an abrupt increase in the pH within a vesicle. This has been shown to have an impact on the activity of hormone-processing enzymes within a vesicle. In chromaffin cells the increase in pH activates the plasminogen activator inhibitor (PAI) contained within the same vesicle, which contains tissue plasminogen

activator (tPA) [57]. When a fusion pore opens, the rise in pH activates PAI. If the fusion pore stays small then tPA is inactivated by the PAI as the two remain in close proximity. However, if the fusion pore expands rapidly then the tPA can escape in a fully active form. Thus, vesicles can serve as nanoscale chemical reaction chambers that alter the composition of secretion. Processing enzymes are often contained within the vesicles harboring their prohormone targets, and it is likely that fusion pores control the time and thus the extent of prohormone processing.

Membrane mixing. A fusion pore can serve as a conduit for the mixing of the vesicle and plasma membrane. A proteinaceous pore essentially blocks mixing, but a lipidic pore provides a fluid membrane pathway for the lateral diffusion of lipid and membrane protein. Single-vesicle capacitance steps have revealed the escape of vesicle membrane during transient fusion pore openings [58]. STED microscopy indicates that a plasma membrane label can flow into a vesicle [32]. For small lipidic pores, membrane mixing should be slow. Membrane mixing can be monitored by loss of membrane label, and efforts have been made to square the observed rate with that expected for fusion pores of different sizes [34]. The onset of lipid mixing pinpoints the time of appearance of lipidic pores and thus marks a critical structural transition in the fusion pore. Since vesicle membranes and plasma membranes differ in their lipid and protein composition, mixing of the membranes adds a challenge to the recycling of vesicle materials and the regeneration/replenishment of vesicles after secretion.

5.3 The energy landscape of membrane fusion

Fusion pore dynamics is shaped by an energy landscape that combines lipid bilayer mechanics and protein conformation. Lipid bilayer elasticity can be studied using continuum models that represent shape-related energies in terms of membrane curvature. Detailed molecular models of lipid bilayers complement this approach. The influence of protein conformation can be studied with the aid of experimental structures and computer models. The energy landscape determines the relative stability of different states and their rates of interconversion, thereby controlling the evolution of a fusion pore along the membrane fusion reaction pathway. Many of the energetic contributions are large and opposing, allowing small imbalances in one direction or the other to drive a fusion pore into different configurations.

Mean curvature of a membrane. Changing the shape of a lipid bilayer membrane changes its energy. Figure 5.2(a) illustrates the rearrangements of phospholipids within a lipid bilayer in the shape of a fusion pore. As the lipids rotate within each monolayer, their head-group and hydrocarbon tail distances change in opposite directions. These complex interactions between lipid molecules in a membrane can be simplified into a continuum description of membrane bending using the theory of elasticity [59, 60]. A point on a surface has two principle curvatures corresponding to two perpendicular arcs through that point (figure 5.2(a)). These arcs have radii R_1 and R_2; R_1 is for the meridian curvature, where the arc is in the plane of the illustration, and R_2 is for the parallel curvature, where the arc is perpendicular to the plane of the illustration (light blue contours in figure 5.2(a) are the arcs and the

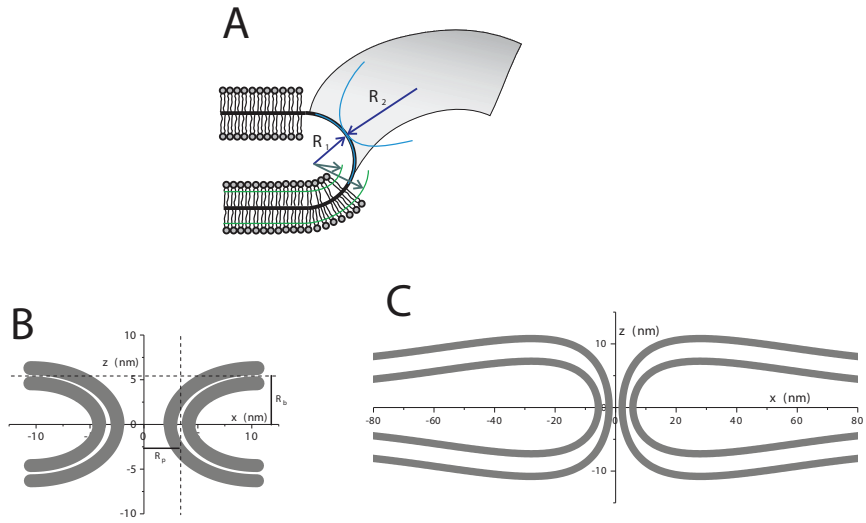

Figure 5.2. Membrane bending in fusion pores. (a) A toroidal lipidic fusion pore formed by a lipid bilayer. The circular in-plane arc has a radius of R_1 and the out-of-plane arc has a radius of R_2. The blue arcs are for the bilayer; the green arcs show the neutral surfaces of the meridian curvature in each monolayer. (b) A minimum bending energy shape of a fusion pore formed by a spatially restricted system. Reproduced with permission from [8]. Copyright © 2009, Springer Nature Switzerland AG. Part of Springer Nature. (c) A minimum bending energy shape of a fusion pore with a greater spatial extent allows bowing (lengthening) [10].

principal radii are dark blue). Figure 5.2(a) illustrates these features with a toroidal shape in which R_1 is constant within the pore. Other shapes are possible.

One of the forms of elastic bending energy at a point on a surface is proportional to the *mean curvature* squared, $\left(\frac{1}{R_1}+\frac{1}{R_1}-C_0\right)^2$, where C_0 is the spontaneous curvature. The total energy arising from mean curvature can be calculated by integrating this quantity over the surface and multiplying by the bending modulus. The lipid bilayer in a fusion pore has especially high curvature. In some regions, R_1 and R_2 can be smaller than the bilayer dimensions. Detailed calculations indicate that the magnitude of this energy is very sensitive to the shape of the fusion pore. C_0 also has an impact, and negative values reduce the energy of a fusion pore [7, 8, 61]. Lipids with negative C_0 promote the fusion of lipid vesicles [62, 63] and accelerate the transition from proteinaceous pores to lipidic pores during exocytosis [64].

For a toroidal fusion pore (figure 5.2(a)) the mean curvature bending energy can be calculated to be 75 kT [61, 65]. However, a toroid is not the shape that minimizes the bending energy. In fact, a well-known result from differential geometry states that a catenoid, which is the surface of revolution formed by a catenary (a hyperbolic cosine function), has zero mean curvature everywhere [66]. Indeed, soap films between two parallel coaxial rings spontaneously assume a catenoid shape [67]. A catenoid has a pore-like overall contour, suggesting that the mean curvature contribution to fusion pore energy can be dismissed as negligible. However, two factors lead to significant membrane bending energies in fusion

pores. One issue is that plasma membranes are generally flat, but catenoids do not have a horizontal limiting surface, so the junction with the plasma membrane must depart from a catenoid shape. Another problem is that a lipid bilayer is formed from two monolayers, each of which has its own neutral surface (in figure 5.2(a), the monolayer neutral surfaces are light green; their meridian curvatures are dark green). The two surfaces cannot each be catenoids, because it is geometrically impossible for two catenoids to be parallel. For distances between the two monolayer neutral surfaces comparable to R_1 and R_2, the deviations from a catenoidal shape must be significant. Minimizing the bending energy of two coupled monolayers yielded values ranging from 11 to 120 kT, with lower values for negative monolayer C_0 [8]. Figure 5.2(b) illustrates a shape that minimizes bending energy with a limited lateral dimension and a basis function that limits shapes to monotonic gradation between vertical and horizontal. Biological membranes have an asymmetric lipid distribution between the two leaflets and this can also reduce the energy cost of forming a fusion pore. Further analysis of energy minimization using both continuum elasticity and coarse-grained molecular dynamics showed that that the energy can be reduced further by a modification of shape in which the pore elongates vertically. Figure 5.2(c) illustrates the minimal shape for minimization of a larger system in which the elongated shape is more striking. This change in shape can reduce the bending energy to low values [9, 10].

Theoretical studies of the membrane bending energy landscape have reached a consensus that a lipidic fusion pore has a minimum energy at a particular diameter, and that expansion of the fusion pore encounters a large energy barrier [7, 8, 61, 68]. This stable pore is supported by the observation of similar sizes when fusion is driven by different numbers of SNARE complexes [51] and by the observation of a metastable plateau in the permeability of late-stage fusion pores seen in amperometry recordings (figure 5.1; [23]). This minimum bending energy state is also likely responsible for the stable fusion pores often seen in capacitance recordings.

The variation in energy with shape has a major impact on fusion pore dynamics. To form a lipidic fusion pore, the two fusing membranes must initially directly contact one another. This means that it is not possible to directly proceed to the lowest-energy shape. An initial fusion pore has a shape that is closer to what is seen when the two membranes are touching (figure 5.2(b)). This initial lipidic pore cannot have a bowing/teardrop shape and must rearrange to reach a global minimum on the membrane bending energy surface (figure 5.2(c)). Thus, the energy landscape defined by mean curvature provides an appealing mechanism for the structural transition of lipidic fusion pores.

Gaussian curvature. In addition to the mean curvature just discussed, elastic membrane bending energy includes another term, Gaussian curvature, equal to $\frac{1}{R_1 R_2}$. Like mean curvature, this quantity can be integrated over a surface and multiplied by a modulus to obtain a contribution to the energy of membrane bending. However, the Gaussian curvature has a remarkable mathematical property: for a given topology, its integral over a surface is invariant with respect to shape [66]. For example, a sphere can be contorted into any arbitrary shape; the mean curvature integral will vary, but as long as the surface completely separates the

inside from the outside, the integral over the Gaussian curvature will not change. This makes Gaussian curvature irrelevant to the above discussion of fusion pore shapes (figure 5.2). However, Gaussian curvature is very relevant to the energetics of fusion pore formation. When a vesicle fuses with the plasma membrane, two spheres become one. The change in topology produces a precise change in the integral over the Gaussian curvature. The change in membrane bending energy is large and positive [69, 70]. This constitutes an important feature of the fusion energy landscape and is predicted to make the energy barrier to the formation of a lipidic fusion pore very high. Fusing the two monolayers sequentially offers an appealing hypothetical mechanism that breaks the process into two easier steps. Because of its topological origin, it has proven difficult to adapt the continuum concept of Gaussian curvature to the molecular scale and incorporate it into models for the rearrangements associated with membrane fusion. At present, there is no satisfactory explanation for how Gaussian curvature impacts the changes at the molecular level that accompany the membrane fusion transition.

Molecular models. Continuum elasticity suffers from the shortcoming of ignoring molecular details. One can overcome this weakness with computational molecular dynamics, but modeling membrane fusion requires a system with a large number of lipid molecules, and this presents a serious obstacle to computer simulations. Although all-atom models have been used to model membrane fusion in very small systems, coarse-grained models of lipid bilayers have been developed for work with larger systems. These studies succeeded in simulating membrane fusion and in capturing intermediates in various stages of exocytosis, including lipidic fusion pores [71–74]. A comparison of coarse-grained, all-atom, and continuum models [10] showed that as energy minimization progressed, each model approached a similar shape, recapitulating the axial lengthening described above for the continuum model (figure 5.2(c)). The convergence of these different theories validated the distinct approaches. A coarse-grained simulation has incorporated the SNARE complex to model the formation of a lipidic fusion pore containing the C-terminal residues of the SNARE TMDs [74]. Coarse-grained models of the fusion of small vesicles led to a fusion pore that expanded rapidly and was not metastable [71, 73, 74]. This contrasts with the theoretical and experimental studies summarized above, which indicated that a narrow pore is a metastable state at a local energy minimum. It is not clear whether the rapid expansion seen in stimulations is behavior unique to small vesicles or a shortcoming of the theory.

SNARE complex zipping. SNARE proteins have general membrane trafficking functions. Most forms of Ca^{2+}-triggered exocytosis are mediated by the vesicle SNARE synaptobrevin and the plasma membrane SNAREs syntaxin and SNAP-25. These three proteins form a complex of exceptionally high stability [75]. SNAREs harbor domains of ~65 amino acids, known as SNARE motifs, which are capable of assembling into a tight bundle of four α-helices (one each from synaptobrevin and syntaxin and two from SNAP-25). With SNARE proteins tethered to the vesicle and plasma membranes, zipping from the membrane's distal N-terminus to the membrane's proximal C-terminus draws the two membranes together [76–78]. The energy released during the formation of this complex is

thought to be strong enough to overcome inter-membrane repulsion, and the stresses produced by assembly can bend and reshape lipid membranes. SNARE complex assembly proceeds in multiple stages [79, 80]. Assembly of the N-terminal, C-terminal, and linker domains of the SNARE motifs are estimated to release an energy of 65 kT [79]. Association of the two TMDs of syntaxin and synaptobrevin could contribute additional energy [81, 82], but this would have to be a late step, as it ends with a fully lipidic pore and places both TMDs in the same lipid membrane. In a proteinaceous pore the TMDs are still in separate membranes, so SNAREs cannot be fully zipped at this point. The distinct stages of SNARE complex assembly could provide driving forces for multiple steps, either leading to the formation of an initial fusion pore or to later pore states. Once assembly has completed, it can play no further role in subsequent transitions involving shape changes of the lipidic pore.

Helix completion. Syntaxin and synaptobrevin are anchored in membranes by a presumably helical TMD. Linkers made from ~11 amino acids connect the TMDs to the ~65 amino acid α-helical SNARE motifs. Assembly of the SNARE motifs up to the linkers leaves two nearly perpendicular α-helical segments in each protein. This creates a disordered break between two helical domains. The cooperativity of the helix–coil transition depends on positive free energy at the helix–coil boundary [5]. This gives rise to a driving force that joins the two helical segments into a single contiguous helix. The two lipid bilayers within which the two TMDs are embedded must merge to complete the helices, so helix completion can be harnessed to drive membrane fusion. This process has been incorporated into a theory for SNARE-mediated membrane fusion that produced rates in the millisecond range [83]. A SNARE complex anchored in a lipid bilayer by the TMD of syntaxin rotates from an orientation parallel to the lipid bilayer to a perpendicular one upon the addition of Ca^{2+}-synaptotagmin. This indicates regulation of the helix completion force [84]. It has been proposed that the rotation of synaptobrevin's TMD encounters an energy barrier due to its interaction with the lipid bilayer, in which the rotation pulls the C-terminus into the hydrocarbon interior and disrupts the bilayer to initiate fusion [85].

SNARE complex number. There have been many efforts to determine how many SNARE complexes participate in exocytosis, and numbers vary widely [16, 86]. Different numbers of SNARE complexes have been implicated in dictating whether a fusion pore is proteinaceous or lipidic [37]. With only one complex, no fusion pore forms and the outcome is hemifusion [87]. A proteinaceous initial fusion pore is anticipated to be larger when greater numbers of SNARE complexes provide more TMDs to line the pore, and the transition rates between different states are also strongly affected [51, 52]. Thus, the SNARE complex number plays an important role in the state of a fusion pore, and may well account for some of the diversity encountered in different studies. This raises interesting questions about whether additional SNARE complexes are recruited as fusion progresses and fusion pores grow, and whether cells control the number of SNARE complexes to choose different modes of secretion. Given the high energetic barrier to fusion pore dilation discussed above, one can speculate that recruiting more SNARE complexes may provide the essential drive for full fusion. Fewer SNARE complexes leave kiss-and-run as the favored option.

Entropy of SNARE pinwheels. The geometric arrangement of SNARE complexes extending outward from a central fusion axis has been termed a 'SNAREpin,' and likened to a pinwheel [46]. An outward, radial movement of the SNARE complexes in this arrangement forces the fusion pore to expand. This outward radial movement increases the rotational entropy, thus providing a driving force for SNARE complex movement away from the fusion pore center [88]. Incorporating this rotational entropy term into a model for fusion pore dilation recapitulated the increased rate of expansion with SNARE complex number [51]. This force is not relevant to the early steps of fusion pore dynamics, but can play an important role in later expansion steps.

Hydrophobic energy. The hydrophobic effect presents an energetic challenge to membrane trafficking. Avoiding hydrocarbon–water contact requires the interiors of two separate bilayers to merge with one another without being exposed to the water between the bilayers. This consideration motivated the introduction of the lipid-stalk model, in which fusion can occur with virtually no hydrocarbon–water contact [65, 89]. Any mechanism for fusion requires careful attention to how much hydrocarbon–water exposure occurs. The hydrophobic energy can be calculated by multiplying the area of water–oil contact by an empirical parameter. Surface tension measurements suggested a value for this parameter of 50 ergs cm^{-2} ~75 cal $Å^{-2}$. Using this value for a cylindrical water-filled pore lined entirely by hydrocarbon gave extremely high energies [89]. Solvent-partitioning measurements suggest a much lower value of 25 cal $Å^{-2}$ for this parameter [90, 91], and of course, using this value, the hydrophobic barrier to membrane fusion was much lower. Limited hydrocarbon–water contact was incorporated into a model of SNARE-mediated fusion driven by helix completion, and the resulting energy barriers were readily surmountable [83]. During the dynamic rearrangements of a lipidic fusion pore, the bilayer maintains its integrity, so the hydrophobic effect is irrelevant. However, fusion pore closure requires a process that reverses the formation of a lipidic pore. The walls of a constricting pore fuse [92], and the advantages of the lipid-stalk model in minimizing hydrophobic contacts are again likely to be relevant.

Hydration forces. Lipid bilayers repel one another due to the hydration energy of the phospholipid head groups [93]. Membranes must overcome this barrier in order to fuse. Puckering of the membrane can reduce this energy by limiting the contact area. Because this force originates from hydration, osmoticants have proven broadly effective in promoting many forms of membrane fusion [94]. The fact that osmoticants are so fusogenic indicates that the hydration force is a major barrier to membrane fusion. Modeling has suggested that membrane repulsion plays a role in opposing the fusion of membranes mediated by SNAREs [51].

Membrane tension. Lateral forces within membranes connect area changes to energy changes and drive lateral membrane movement. Membrane tension can drive fusion pore expansion by changing the area of the cell surface [95]. Tension promotes the fusion of lipid bilayers [96] and fusion pore expansion during exocytosis [97]. However, the initial fusion pores are small, and their very small area limits the impact of tension on their dynamics. Thus, membrane tension is likely to play a role in the later steps of fusion pore dynamics, rather than the earlier steps.

5.4 Fusion pore states

Fusion pores change their properties as they advance along the fusion reaction pathway. In many cases the boundaries between states seem blurred and methodological differences leave questions about how to make comparisons. Amperometry reveals the earliest, briefest states, while capacitance and imaging techniques reveal later, more stable states. Different techniques often reveal roughly similar sequences, albeit with different timescales. Pores assume an initial state, expand, and constrict; the final outcomes of closure, prolonged stasis, expansion, or collapse appear to vary widely. Some consistent trends can be discerned, some of the changes can be interpreted in terms of the energy landscape, and some classifications of different fusion pore states can be attempted.

Nascent pore. The critical opening transition generates a nascent fusion pore. This initial pore is necessarily small, as fusion starts out as a highly focused localized event. As noted above, the nascent pore produces a prespike foot in amperometry recordings [14, 15, 98, 99]. The prespike foot appears to be stable for milliseconds, but it is not entirely clear how stable it really is. Published recordings show prespike feet as approximately flat, with varying degrees of upward slope. The mean amplitudes of kiss-and-run events are uncorrelated with duration, arguing against growth [100, 101]. If expansion is indeed occurring, it is much slower than the expansion that marks the onset of the amperometric spike. The lifetimes of prespike feet vary stochastically, and distributions are exponential [99, 100, 102] or an exponential–Gaussian convolution [64]. Thus, the early transitions are Markov processes, recalling the kinetics of ion-channel gating [103]. The Markov picture supported by exponential lifetime distributions is not consistent with the slow expansion just discussed, as a Markov process implies stability prior to exit.

Fusion pore conductances fall within the range of ion-channel conductances, supporting the view of proteinaceous fusion pores [104, 105]. The ion-channel analogy is further supported by studies of prespike feet and SNARE TMD mutations. Tryptophan substitutions at key TMD residues reduce catecholamine flux through the nascent fusion pore, glycine substitution increases catecholamine flux, and charge substitutions alter flux in a manner consistent with electrostatic interactions [17–19]. These results indicate an intimate relation between the fusion pore and the SNARE TMDs. Figure 5.3 highlights the residues within the syntaxin and synaptobrevin TMDs implicated by amperometry experiments as pore liners. Flux perturbation studies in other experimental systems implicate these and other residues in fusion pores [37, 38], and these are also highlighted in figure 5.3. However, in these other studies, it is not as clear that the fusion pores are nascent, i.e. at the earliest time after opening.

Larger vesicles produce prespike feet with longer lifetimes. The greater stability of the nascent pore can be accounted for by variations in the amount of curved lipid bilayer created within the lipidic fusion pore (figure 5.2) when a nascent fusion pore expands [64]. This indicates that there is very little lipid bilayer curvature in the nascent pore, thus supporting a greater role for protein than lipid.

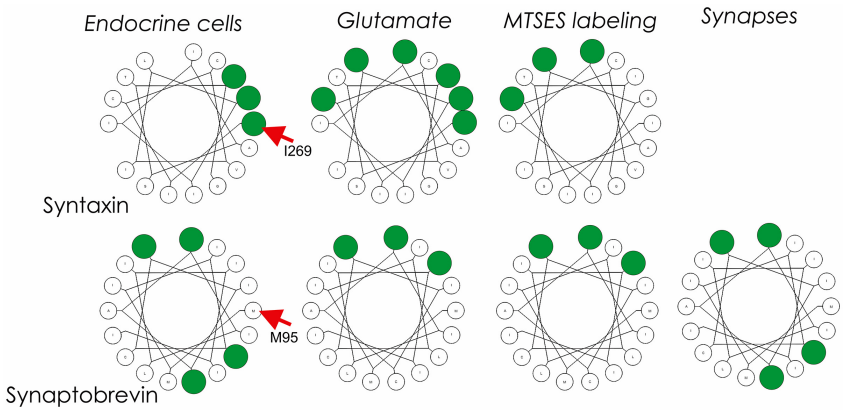

Figure 5.3. Helical wheels highlight SNARE TMD residues in initial fusion pores. The residues were implicated by amperometry and capacitance with mutants of syntaxin [19] and synaptobrevin [17], by glutamate flux and cysteine accessibility (MTSES labeling) in reconstituted fusion pores [37], and by glutamate flux through synaptic fusion pores [38]. Red arrowheads indicate the N-terminal residue of the TMDs. Modified from [16].

Capacitance recording reveals opening transitions, but with lower time resolution than amperometry recording. Nevertheless, tryptophan mutations in SNARE TMDs alter the conductance of fusion pores [17, 19]. The initial fusion pores seen in capacitance recordings appear more stable than prespike feet, with lifetimes that are one or two orders of magnitude longer. Because of the difference in the time resolutions of capacitance and amperometry, it is not clear that they are viewing the same structure. Indeed, amperometry recording suggests that the capacitance measurements correspond to the later plateau in permeability (figure 5.1) [23].

Nascent fusion pores can close, indicating that this state is an important bifurcation point. Expansion is the other possible outcome. The initial transition from a closed pore to an open pore is a clear and functionally important transition that can be controlled by a host of molecules and conditions [39]. Likewise, the branch point between expansion and closure and the stability of the nascent pore are influenced by many factors. Thus, the initial state of the fusion pathway is an important focus of biological control.

Early expansion. A nascent fusion pore can expand to accelerate flux, and this expansion is especially clear at the onset of an amperometric spike. This expansion likely entails infiltration of a proteinaceious pore with lipid [83, 104] and delivery of the fusion pore into the lipid membrane bending energy surface. However, as discussed above, the first lipidic form taken by a fusion pore is not necessarily at a minimum in membrane bending energy. This depends on the nature of the transition and the shape that is most easily accessed [8]. Thus, early expansion generates an unstable transient structure, and the shape then moves to a minimum on the membrane bending energy surface (figure 5.1) [23]. The early permeability peak in this plot can be viewed as an unstable transition state between two metastable states. The expanded pore may have very high permeability, but its short duration limits

the amount of vesicle content loss. Brief spike-like upticks have been observed during prespike feet, which are likely to be abortive starts to this initial expansion process [98].

Constriction. The rapid constriction following the permeability peak brings a fusion pore into a new stable state (figure 5.1). This dynamic process likely reflects the movement of the lipidic pore along the membrane bending landscape, and the pore becomes stable upon arriving at the energy minimum. The plateau in permeability can thus provide information about the nature of this lipidic pore and offers the hope of pointing to the shape a lipidic pore actually assumes (such as figures 5.2(b) and (c)). Amperometry indicates that this state remains stable for a minimum of several tens of milliseconds. During this time the entire content of catecholamine escapes. The retention of fluorescent content [29], preservation of vesicle shape [32], and sustained membrane deformation [106] for times of the order of seconds all support the existence of a stable constricted pore at the membrane bending energy minimum.

The constricted pore is an important focus of biological control [23]. Of the many candidate regulators, dynamin merits special mention. It forms collars around lipid tubules [107, 108] and influences the decay of amperometric spikes [109–111]. This action of dynamin suggests that it bends the membrane to regulate the shape of the narrow lipidic fusion pore. The action of dynamin is regulated by calcineurin dephosphorylation and syndapin/N-WASP signaling [112]. Other proteins that influence spike shape and presumably regulate late-stage fusion pores include myosin [113], Cdc42 [97], complexin [114], and Munc18 [115]. Focusing so many forms of regulation on this state speaks to its importance in controlling the speed, selectivity, and extent of content release.

Late-stage expansion and vesicle collapse. Electron micrographs reveal fusing vesicles in various stages of collapse [116–118]. Tracking the time course of conductance indicates that fusion pores can expand after opening [56]. In human neutrophils, once the conductance growth surpasses ~ 1 nS the pores pass a point of no return and commit to full fusion [119]. With large vesicles of beige mouse mast cells, membrane flows through a fluid lipidic fusion pore [58], indicating the onset of collapse of the vesicle membrane into the plasma membrane. In pancreatic islets the growth of fusion pores can be tracked as a vesicle collapses by following the passage of markers with increasing sizes [120]. Polarization TIRF microscopy [30] and STED microscopy [32] indicate that some fusion events progress to vesicle collapse. The transition to full fusion varies with biological conditions. Intense electrical activity increases the likelihood of full fusion in chromaffin cells [53], while cAMP controls this transition in pancreatic β cells [54]. Dynamin [121] and actin [122] also play a role in destabilizing the constricted pore so that it can expand to enable vesicle collapse. Full fusion and vesicle collapse play an important role in determining whether large peptides are retained or released, and the many forms of control over this process attest to the importance of vesicle collapse in controlling secretion.

Closure. Essentially all of the techniques for visualizing single fusion pores have detected some form of partial, subquantal release, thus implying fusion pore closure. Membrane capacitance increases in steps during vesicle fusion, and upward steps are

often followed within a second or less by a downward step of the same size [1, 2, 12, 123]. The tight temporal correlation between the upward and downward steps suggests that the fusion pore can close soon after opening in a kiss-and-run process. Amperometry indicates that very small, nascent fusion pores can close [100, 101, 124]. Some spikes might be terminated by the closure of larger, late-stage pores [125]. Fluorescent content loss [126] and membrane label loss [26, 27] often appear limited. Pores can reach quite large sizes before closing without vesicle collapse [32]. Thus, closure is not limited to a single fusion pore state. Multiple states appear to be capable of closing and it is likely that the underlying mechanisms differ widely.

Small amperometric events with amplitudes roughly comparable to prespike feet often terminate without a spike. These 'stand-alone feet' are thought to report kiss-and-run events in which a fusion pore closes rather than expands [100, 101, 127]. Endocrine cells can also produce very small stand-alone feet that never terminate with a spike [124]. These events may represent a form of exocytosis controlled by a small fusion pore that cannot expand. The closure of these nascent proteinaceous pores is reminiscent of ion-channel gating, but late-stage closure is very different because the pore is lipidic. This form of closure can actually be visualized in mechanistic terms similar to those hypothesized for lipid bilayer fusion. As the lipid bilayer surrounding a fission pore narrows, the walls approach one another, push head groups away, and drive the formation of a stalk-like structure similar to that hypothesized for fusion [92]. In a sense, during fission, the pore walls fuse. This process may be driven by the compression of a surrounding protein collar such as that formed by dynamin.

5.5 Conclusions

Studies of fusion pores have provided insight into the mechanism of exocytosis. Although the divergent fusion pore behavior in the literature can appear confusing, the diversity actually offers the key to unlocking the mysteries of protein control. The different states of fusion pores highlight pathways taken by biological membranes during fusion. The membrane fusion reaction pathway proceeds through a sequence of fusion pore structures, each with distinct properties and functions. With the discoveries of multiple fusion pore states that interconvert dynamically, a framework is starting to emerge that can guide researchers in further studies of the mechanism of exocytosis.

References

[1] Neher E and Marty A 1982 Discrete changes of cell membrane capacitance observed under conditions of enhanced secretion in bovine adrenal chromaffin cells *Proc. Natl Acad. Sci. USA* **79** 6712–6

[2] Fernandez J M, Neher E and Gomperts B D 1984 Capacitance measurements reveal stepwise fusion events in degranulating mast cells *Nature* **312** 453–5

[3] Zimmerberg J, Curran M, Cohen F S and Brodwick M 1987 Simultaneous electrical and optical measurements show that membrane fusion precedes secretory granule swelling during exocytosis of beige mouse mast cells *Proc. Natl Acad. Sci. USA* **84** 1585–9

[4] Breckenridge L J and Almers W 1987 Currents through the fusion pore that forms during exocytosis of a secretory granule *Nature* **328** 814–7
[5] Jackson M B 2006 *Molecular and Cellular Biophysics* (Cambridge: Cambridge University Press)
[6] Hille B 1992 *Ion Channels of Excitable Membranes* (Sunderland: Sinauer)
[7] Nanavati C, Markin V S, Oberhauser A F and Fernandez J M 1992 The exocytotic fusion pore modeled as a lipidic pore *Biophys. J.* **63** 1118–32
[8] Jackson M B 2009 Minimum membrane bending energies of fusion pores *J. Membr. Biol.* **231** 101–15
[9] Ryham R J, Ward M A and Cohen F S 2013 Teardrop shapes minimize bending energy of fusion pores connecting planar bilayers *Phys. Rev. E Stat. Nonlin. Soft Matter Phys.* **88** 062701
[10] Yoo J, Jackson M B and Cui Q 2013 A comparison of coarse-grained and continuum models for membrane bending in lipid bilayer fusion pores *Biophys. J.* **104** 841–52
[11] Lindau M and Alvarez de Toledo G 2003 The fusion pore biochim *Biophys. Acta* **1641** 167–73
[12] Klyachko V A and Jackson M B 2002 Capacitance steps and fusion pores of small and large-dense-core vesicles in nerve terminals *Nature* **418** 89–92
[13] Wightman R M, Jankowski J A, Kennedy R T, Kawagoe K T, Schroeder T J, Leszczyszyn D J, Near J A, Diliberto D J Jr and Viveros O H 1991 Temporally resolved catecholamine spikes correspond to single vesicle release from individual chromaffin cells *Proc. Natl Acad. Sci. USA* **88** 10754–8
[14] Chow R H, von Rüden L and Neher E 1992 Delay in vesicle fusion revealed by electrochemical monitoring of single secretory events in adrenal chromaffin cells *Nature* **356** 60–3
[15] Jankowski J A, Schroeder T J, Ciolkowski E L and Wightman R M 1993 Temporal characteristics of quantal secretion of catecholamines from adrenal medullary cells *J. Biol. Chem.* **268** 14694–700
[16] Chang C W, Chiang C W and Jackson M B 2017 Fusion pores and their control of neurotransmitter and hormone release *J. Gen. Physiol.* **149** 301–22
[17] Chang C W, Hui E, Bai J, Bruns D, Chapman E R and Jackson M B 2015 A structural role for the synaptobrevin 2 transmembrane domain in dense-core vesicle fusion pores *J. Neurosci.* **35** 5772–80
[18] Han X and Jackson M B 2005 Electrostatic interactions between the syntaxin membrane anchor and neurotransmitter passing through the fusion pore *Biophys. J.* **88** L20–2
[19] Han X, Wang C T, Bai J, Chapman E R and Jackson M B 2004 Transmembrane segments of syntaxin line the fusion pore of Ca^{2+}-triggered exocytosis *Science* **304** 289–92
[20] Wightman R M, Schroeder T J, Finnegan J M, Ciolkowski E L and Pihel K 1995 Time course of release of catecholamines from individual vesicles during exocytosis at adrenal medullary cells *Biophys. J.* **68** 383–90
[21] Schroeder T J, Borges R, Finnegan J M, Pihel K, Amatore C and Wightman R M 1996 Temporally resolved, independent stages of individual exocytotic secretion events *Biophys. J.* **70** 1061–8
[22] Wightman R M, Dominguez N and Borges R 2018 How intravesicular composition affects exocytosis *Pflugers Arch.* **470** 135–41
[23] Jackson M B, Hsiao Y T and Chang C W 2020 Fusion pore expansion and contraction during catecholamine release from endocrine cells *Biophys. J.* **119** 219–31

[24] Ryan T A, Reuter H and Smith S J 1997 Optical detection of a quantal presynaptic membrane turnover *Nature* **388** 478–82
[25] Zenisek D, Steyer J A, Feldman M E and Almers W 2002 A membrane marker leaves synaptic vesicles in milliseconds after exocytosis in retinal bipolar cells *Neuron* **35** 1085–97
[26] Aravanis A M, Pyle J L and Tsien R W 2003 Single synaptic vesicles fusing transiently and successively without loss of identity *Nature* **423** 643–7
[27] Richards D A, Bai J and Chapman E R 2005 Two modes of exocytosis at hippocampal synapses revealed by rate of FM1–43 efflux from individual vesicles *J. Cell Biol.* **168** 929–39
[28] Taraska J W and Almers W 2004 Bilayers merge even when exocytosis is transient *Proc. Natl Acad. Sci. USA* **101** 8780–5
[29] Tsuboi T, McMahon H T and Rutter G A 2004 Mechanisms of dense core vesicle recapture following 'kiss and run' ('cavicapture') exocytosis in insulin-secreting cells *J. Biol. Chem.* **279** 47115–24
[30] Anantharam A, Onoa B, Edwards R H, Holz R W and Axelrod D 2010 Localized topological changes of the plasma membrane upon exocytosis visualized by polarized TIRFM *J. Cell Biol.* **188** 415–28
[31] Anantharam A, Axelrod D and Holz R W 2012 Real-time imaging of plasma membrane deformations reveals pre-fusion membrane curvature changes and a role for dynamin in the regulation of fusion pore expansion *J. Neurochem.* **122** 661–71
[32] Shin W, Ge L, Arpino G, Villarreal S A, Hamid E, Liu H, Zhao W D, Wen P J, Chiang H C and Wu L G 2018 Visualization of membrane pore in live cells reveals a dynamic-pore theory governing fusion and endocytosis *Cell* **173** 934–45 e12
[33] Zhao W D, Hamid E, Shin W, Wen P J, Krystofiak E S, Villarreal S A, Chiang H C, Kachar B and Wu L G 2016 Hemi-fused structure mediates and controls fusion and fission in live cells *Nature* **534** 548–52
[34] Abbineni P S, Axelrod D and Holz R W 2018 Visualization of expanding fusion pores in secretory cells *J. Gen. Physiol.* **150** 1640–6
[35] Pawlu C, DiAntonio A and Heckmann M 2004 Postfusional control of quantal current shape *Neuron* **42** 607–18
[36] Guzman R E, Schwarz Y N, Rettig J and Bruns D 2010 SNARE force synchronizes synaptic vesicle fusion and controls the kinetics of quantal synaptic transmission *J. Neurosci.* **30** 10272–81
[37] Bao H, Goldschen-Ohm M, Jeggle P, Chanda B, Edwardson J M and Chapman E R 2016 Exocytotic fusion pores are composed of both lipids and proteins *Nat. Struct. Mol. Biol.* **23** 67–73
[38] Chiang C W, Chang C W and Jackson M B 2018 The transmembrane domain of synaptobrevin influences neurotransmitter flux through synaptic fusion pores *J. Neurosci.* **38** 7179–91
[39] Chiang C W, Shu W C, Wan J, Weaver B A and Jackson M B 2021 Recordings from neuron-HEK cell cocultures reveal the determinants of miniature excitatory postsynaptic currents *J. Gen. Physiol.* **153** e202012849
[40] Khanin R, Parnas H and Segel L 1994 Diffusion cannot govern the discharge of neurotransmitter in fast synapses *Biophys. J.* **67** 966–72
[41] Clements J D 1996 Transmitter timecourse in the synaptic cleft: its role in central synaptic function *Trends Neurosci.* **19** 163–71

[42] Stiles J R, Van Helden D, Bartol T M, Salpeter E E and Salpeter M M 1996 Miniature endplate current rise times <100 μs from improved dual recordings can be modeled with passive acetylcholine diffusion from a synaptic vesicle *Proc. Natl Acad. Sci. USA* **93** 5747–52
[43] Jackson M B 2007 In search of the fusion pore of exocytosis *Biophys. Chem.* **126** 201–8
[44] He L, Wu X-S, Mohan R and Wu L-G 2006 Two modes of fusion pore opening revealed by cell-attached recordings at a synapse *Nature* **444** 102–5
[45] Richards D A 2009 Vesicular release mode shapes the postsynaptic response at hippocampal synapses *J. Physiol.* **587** 5073–80
[46] Weber T, Zemelman B V, McNew J A, Westermann B, Gmachl M, Parlati F, Sollner T H and Rothman J E 1998 SNAREpins: minimal machinery for membrane fusion *Cell* **92** 759–72
[47] Jackson M B and Chapman E R 2006 Fusion pores and fusion machines in Ca^{2+}-triggered exocytosis *Annu. Rev. Biophys. Biomol. Struct.* **35** 135–60
[48] Karatekin E 2018 Toward a unified picture of the exocytotic fusion pore *FEBS Lett.* **592** 3563–85
[49] Shi L, Shen Q T, Kiel A, Wang J, Wang H W, Melia T J, Rothman J E and Pincet F 2012 SNARE proteins: one to fuse and three to keep the nascent fusion pore open *Science* **335** 1355–9
[50] Wu Z, Auclair S M, Bello O, Vennekate W, Dudzinski N R, Krishnakumar S S and Karatekin E 2016 Nanodisc-cell fusion: control of fusion pore nucleation and lifetimes by SNARE protein transmembrane domains *Sci. Rep.* **6** 27287
[51] Wu Z, Bello O D, Thiyagarajan S, Auclair S M, Vennekate W, Krishnakumar S S, O'Shaughnessy B and Karatekin E 2017 Dilation of fusion pores by crowding of SNARE proteins *eLife* **6** e22964
[52] Bao H, Das D, Courtney N A, Jiang Y, Briguglio J S, Lou X, Roston D, Cui Q, Chanda B and Chapman E R 2018 Dynamics and number of trans-SNARE complexes determine nascent fusion pore properties *Nature* **554** 260–3
[53] Fulop T, Radabaugh S and Smith C 2005 Activity-dependent differential transmitter release in mouse adrenal chromaffin cells *J. Neurosci.* **25** 7324–32
[54] MacDonald P E, Braun M, Galvanovskis J and Rorsman P 2006 Release of small transmitters through kiss-and-run fusion pores in rat pancreatic beta cells *Cell Metab.* **4** 283–90
[55] Delacruz J B, Sharma S, Rathore S S, Huang M, Lenz J S and Lindau M 2021 Fusion pores with low conductance are cation selective *Cell Rep.* **36** 109580
[56] Spruce A E, Breckenridge L J, Lee A K and Almers W 1990 Properties of the fusion pore that forms during exocytosis of a mast cell secretory granule *Neuron* **4** 643–54
[57] Bohannon K P, Bittner M A, Lawrence D A, Axelrod D and Holz R W 2017 Slow fusion pore expansion creates a unique reaction chamber for co-packaged cargo *J. Gen. Physiol.* **149** 921–34
[58] Monck J R, Alvarez de Toledo G and Fernandez J M 1990 Tension in secretory granule membranes causes extensive membrane transfer through the exocytotic fusion pore *Proc. Natl Acad. Sci. USA* **87** 7804–8
[59] Boal D 2002 *Mechanics of the Cell* (Cambridge: Cambridge University Press)
[60] Helfrich W 1973 Elastic properties of lipid bilayers: theory and possible experiments *Z. Naturforsch.* C **28** 693–703

[61] Chizmadzhev Y A, Cohen F S, Shcherbakov A and Zimmerberg J 1995 Membrane mechanics can account for fusion pore dilation in stages *Biophys. J.* **69** 2489–500
[62] Chernomordik L, Chanturiya A, Green J and Zimmerberg J 1995 The hemifusion intermediate and its conversion to complete fusion: regulation by membrane composition *Biophys. J.* **69** 922–9
[63] Haque M E and Lentz B R 2004 Roles of curvature and hydrophobic interstice energy in fusion: studies of lipid perturbant effects *Biochemistry* **43** 3507–17
[64] Zhang Z and Jackson M B 2010 Membrane bending energy and fusion pore kinetics in Ca(2+)-triggered exocytosis *Biophys. J.* **98** 2524–34
[65] Kozlov M M, Leikin S L, Chernomordik L V, Markin V S and Chizmadzhev Y A 1989 Stalk mechanism of vesicle fusion. intermixing of aqueous contents *Eur. Biophys. J.* **17** 121–9
[66] Kreyszig E 1991 *Differential Geometry* (New York: Dover)
[67] Ito M and Sato T 2010 *In situ* observation of a soap-film catenoid—a simple educational physics experiment *Eur. J. Phys.* **31** 357–65
[68] Katsov K, Muller M and Schick M 2004 Field theoretic study of bilayer membrane fusion. I. Hemifusion mechanism *Biophys. J.* **87** 3277–90
[69] Siegel D P 2008 The Gaussian curvature elastic energy of intermediates in membrane fusion *Biophys. J.* **95** 5200–15
[70] Hu M, Briguglio J J and Deserno M 2012 Determining the Gaussian curvature modulus of lipid membranes in simulations *Biophys. J.* **102** 1403–10
[71] Kasson P M, Kelley N W, Singhal N, Vrljic M, Brunger A T and Pande V S 2006 Ensemble molecular dynamics yields submillisecond kinetics and intermediates of membrane fusion *Proc. Natl Acad. Sci. USA* **103** 11916–21
[72] Risselada H J and Grubmuller H 2012 How SNARE molecules mediate membrane fusion: recent insights from molecular simulations *Curr. Opin. Struct. Biol.* **22** 187–96
[73] Risselada H J, Kutzner C and Grubmuller H 2011 Caught in the act: visualization of SNARE-mediated fusion events in molecular detail *ChemBioChem* **12** 1049–55
[74] Sharma S and Lindau M 2018 Molecular mechanism of fusion pore formation driven by the neuronal SNARE complex *Proc. Natl Acad. Sci. USA* **115** 12751–6
[75] Hayashi T, McMahon H, Yamasaki S, Binz T, Hata Y, Sudhof T C and Niemann H 1994 Synaptic vesicle membrane fusion complex: action of clostridial neurotoxins on assembly *EMBO J.* **13** 5051–61
[76] Hanson P I, Roth R, Morisaki H, Jahn R and Heuser J E 1997 Structure and conformational changes in NSF and its membrane receptor complexes visualized by quick-freeze/deep-etch electron microscopy *Cell* **90** 523–35
[77] Sorensen J B, Wiederhold K, Muller E M, Milosevic I, Nagy G, de Groot B L, Grubmuller H and Fasshauer D 2006 Sequential N- to C-terminal SNARE complex assembly drives priming and fusion of secretory vesicles *EMBO J.* **25** 955–66
[78] Xu T, Rammner B, Margittai M, Artalejo A R, Neher E and Jahn R 1999 Inhibition of SNARE complex assembly differentially affects kinetic components of exocytosis *Cell* **99** 713–22
[79] Gao Y, Zorman S, Gundersen G, Xi Z, Ma L, Sirinakis G, Rothman J E and Zhang Y 2012 Single reconstituted neuronal SNARE complexes zipper in three distinct stages *Science* **337** 1340–3
[80] Melia T J, Weber T, McNew J A, Fisher L E, Johnston R J, Parlati F, Mahal L K, Sollner T H and Rothman J E 2002 Regulation of membrane fusion by the membrane-proximal coil of the t-SNARE during zippering of SNAREpins *J. Cell Biol.* **158** 929–40

[81] Ellena J F, Liang B, Wiktor M, Stein A, Cafiso D S, Jahn R and Tamm L K 2009 Dynamic structure of lipid-bound synaptobrevin suggests a nucleation-propagation mechanism for trans-SNARE complex formation *Proc. Natl Acad. Sci. USA* **106** 20306–11
[82] Stein A, Weber G, Wahl M C and Jahn R 2009 Helical extension of the neuronal SNARE complex into the membrane *Nature* **460** 525–8
[83] Jackson M B 2010 SNARE complex zipping as a driving force in the dilation of proteinaceous fusion pores *J. Membr. Biol.* **235** 89–100
[84] Kiessling V, Kreutzberger A J B, Liang B, Nyenhuis S B, Seelheim P, Castle J D, Cafiso D S and Tamm L K 2018 A molecular mechanism for calcium-mediated synaptotagmin-triggered exocytosis *Nat. Struct. Mol. Biol.* **25** 911–7
[85] Lindau M, Hall B A, Chetwynd A, Beckstein O and Sansom M S 2012 Coarse-grain simulations reveal movement of the synaptobrevin C-terminus in response to piconewton forces *Biophys. J.* **103** 959–69
[86] Sharma S and Lindau M 2018 The fusion pore, 60 years after the first cartoon *FEBS Lett.* **592** 3542–62
[87] Giraudo C G, Hu C, You D, Slovic A M, Mosharov E V, Sulzer D, Melia T J and Rothman J E 2005 SNAREs can promote complete fusion and hemifusion as alternative outcomes *J. Cell Biol.* **170** 249–60
[88] Mostafavi H, Thiyagarajan S, Stratton B S, Karatekin E, Warner J M, Rothman J E and O'Shaughnessy B 2017 Entropic forces drive self-organization and membrane fusion by SNARE proteins *Proc. Natl Acad. Sci. USA* **114** 5455–60
[89] Chernomordik L V and Kozlov M M 2003 Protein-lipid interplay in fusion and fission of biological membranes *Annu. Rev. Biochem.* **72** 175–207
[90] Jackson M B 2016 The hydrophobic effect in solute partitioning and interfacial tension *Sci. Rep.* **6** 19265
[91] Tanford C 1979 Interfacial free energy and the hydrophobic effect *Proc. Natl Acad. Sci. USA* **76** 4175–6
[92] Kozlovsky Y and Kozlov M M 2003 Membrane fission: model for intermediate structures *Biophys. J.* **85** 85–96
[93] Leikin S, Parsegian V A, Rau D C and Rand R P 1993 Hydration forces *Annu. Rev. Phys. Chem.* **44** 369–95
[94] Lentz B R 1994 Polymer-induced membrane fusion: potential mechanism and relation to cell fusion events *Chem. Phys. Lipids* **73** 91–106
[95] Kozlov M M and Chernomordik L V 2015 Membrane tension and membrane fusion *Curr. Opin. Struct. Biol.* **33** 61–7
[96] Chanturiya A, Chernomordik L V and Zimmerberg J 1997 Flickering fusion pores comparable with initial exocytotic pores occur in protein-free phospholipid bilayers *Proc. Natl Acad. Sci. USA* **94** 14423–8
[97] Bretou M *et al* 2014 Cdc42 controls the dilation of the exocytotic fusion pore by regulating membrane tension *Mol. Biol. Cell* **25** 3195–209
[98] Zhou Z, Misler S and Chow R H 1996 Rapid fluctuations in transmitter release from single vesicles in bovine adrenal chromaffin cells *Biophys. J.* **70** 1543–52
[99] Wang C-T, Grishanin R, Earles C A, Chang P-Y, Martin T F J, Chapman E R and Jackson M B 2001 Synaptotagmin modulation of fusion pore kinetics in regulated exocytosis of dense-core vesicles *Science* **294** 1111–5

[100] Chiang N, Hsiao Y T, Yang H J, Lin Y C, Lu J C and Wang C T 2014 Phosphomimetic mutation of cysteine string protein-alpha increases the rate of regulated exocytosis by modulating fusion pore dynamics in PC12 cells *PLoS One* **9** e99180
[101] Wang C T, Bai J, Chang P Y, Chapman E R and Jackson M B 2006 Synaptotagmin-Ca^{2+} triggers two sequential steps in regulated exocytosis in rat PC12 cells: fusion pore opening and fusion pore dilation *J. Physiol.* **570** 295–307
[102] Bai J, Wang C T, Richards D A, Jackson M B and Chapman E R 2004 Fusion pore dynamics are regulated by synaptotagmin*t-SNARE interactions *Neuron* **41** 929–42
[103] Jackson M B 1992 Stationary single channel analysis *Methods Enzymol.* **207** 729–46
[104] Almers W 1990 Exocytosis *Annu. Rev. Physiol.* **52** 607–24
[105] Lindau M and Almers W 1995 Structure and function of fusion pores in exocytosis and ectoplasmic membrane fusion *Curr. Opin. Cell Biol.* **7** 509–17
[106] Llobet A, Wu M and Lagnado L 2008 The mouth of a dense-core vesicle opens and closes in a concerted action regulated by calcium and amphiphysin *J. Cell Biol.* **182** 1017–28
[107] Hinshaw J E and Schmid S L 1995 Dynamin self-assembles into rings suggesting a mechanism for coated vesicle budding *Nature* **374** 190–2
[108] Bashkirov P V, Akimov S A, Evseev A I, Schmid S L, Zimmerberg J and Frolov V A 2008 GTPase cycle of dynamin is coupled to membrane squeeze and release, leading to spontaneous fission *Cell* **135** 1276–86
[109] Gonzalez-Jamett A M *et al* 2013 Dynamin-2 regulates fusion pore expansion and quantal release through a mechanism that involves actin dynamics in neuroendocrine chromaffin cells *PLoS One* **8** e70638
[110] Trouillon R and Ewing A G 2013 Amperometric measurements at cells support a role for dynamin in the dilation of the fusion pore during exocytosis *ChemPhysChem* **14** 2295–301
[111] Wu Q, Zhang Q, Liu B, Li Y, Wu X, Kuo S, Zheng L, Wang C, Zhu F and Zhou Z 2019 Dynamin 1 restrains vesicular release to a subquantal mode in mammalian adrenal chromaffin cells *J. Neurosci.* **39** 199–211
[112] Samasilp P, Chan S A and Smith C 2012 Activity-dependent fusion pore expansion regulated by a calcineurin-dependent dynamin-syndapin pathway in mouse adrenal chromaffin cells *J. Neurosci.* **32** 10438–47
[113] Neco P, Fernandez-Peruchena C, Navas S, Gutierrez L M, de Toledo G A and Ales E 2008 Myosin II contributes to fusion pore expansion during exocytosis *J. Biol. Chem.* **283** 10949–57
[114] Archer D A, Graham M E and Burgoyne R D 2002 Complexin regulates the closure of the fusion pore during regulated vesicle exocytosis *J. Biol. Chem.* **277** 18249–52
[115] Barclay J W 2008 Munc-18-1 regulates the initial release rate of exocytosis *Biophys. J.* **94** 1084–93
[116] Heuser J E and Reese T S 1981 Structural changes after transmitter release at the frog neuromuscular junction *J. Cell Biol.* **88** 564–80
[117] Torri-Tarelli F, Grohovaz F, Fesce R and Ceccarelli B 1985 Temporal coincidence between synaptic vesicle fusion and quantal secretion of acetylcholine *J. Cell Biol.* **101** 1386–99
[118] Watanabe S 2016 Flash-and-freeze: coordinating optogenetic stimulation with rapid freezing to visualize membrane dynamics at synapses with millisecond resolution *Front Synaptic Neurosci.* **8** 24
[119] Lollike K, Borregaard N and Lindau M 1998 Capacitance flickers and pseudoflickers of small granules, measured in the cell-attached configuration *Biophys. J.* **75** 53–9

[120] Takahashi N, Kishimoto T, Nemoto T, Kadowaki T and Kasai H 2002 Fusion pore dynamics and insulin granule exocytosis in the pancreatic islet *Science* **297** 1349–52
[121] Anantharam A, Bittner M A, Aikman R L, Stuenkel E L, Schmid S L, Axelrod D and Holz R W 2011 A new role for the dynamin GTPase in the regulation of fusion pore expansion *Mol. Biol. Cell* **22** 1907–18
[122] Wen P J *et al* 2016 Actin dynamics provides membrane tension to merge fusing vesicles into the plasma membrane *Nat. Commun.* **7** 12604
[123] Alvarez de Toledo G, Fernandez-Chacon R and Fernandez J M 1993 Release of secretory products during transient vesicle fusion *Nature* **363** 554–8
[124] Wang C T, Lu J C, Bai J, Chang P Y, Martin T F, Chapman E R and Jackson M B 2003 Different domains of synaptotagmin control the choice between kiss-and-run and full fusion *Nature* **424** 943–7
[125] Mellander L J, Trouillon R, Svensson M I and Ewing A G 2012 Amperometric post spike feet reveal most exocytosis is via extended kiss-and-run fusion *Sci. Rep.* **2** 907
[126] Perrais D, Kleppe I C, Taraska J W and Almers W 2004 Recapture after exocytosis causes differential retention of protein in granules of bovine chromaffin cells *J. Physiol.* **560** 413–28
[127] Chang C W, Hsiao Y T and Jackson M B 2021 Synaptophysin regulates fusion pores and exocytosis mode in chromaffin cells *J. Neurosci.* **41** 3563–78